International Journal of Pharmaceutics 404 (2011) 238–249

Contents lists available at ScienceDirect

International Journal of Pharmaceutics

journal homepage: www.elsevier.com/locate/ijpharm

Pharmaceutical Nanotechnology

Development and *in vitro* characterization of paclitaxel and docetaxel loaded into hydrophobically derivatized hyperbranched polyglycerols

C. Mugabe[a], R.T. Liggins[b], D. Guan[b], I. Manisali[b], I. Chafeeva[c], D.E. Brooks[c,d], M. Heller[b], J.K. Jackson[a], H.M. Burt[a,*]

[a] Division of Pharmaceutics and Biopharmaceutics, Faculty of Pharmaceutical Sciences, University of British Columbia, Vancouver, BC, Canada V6T 1Z3
[b] The Centre for Drug Research and Development, Vancouver, BC, Canada
[c] Centre for Blood Research, University of British Columbia, Vancouver, BC, Canada
[d] Departments of Pathology & Laboratory Medicine and Chemistry, University of British Columbia, Vancouver, BC, Canada

ARTICLE INFO

Article history:
Received 19 July 2010
Received in revised form 3 November 2010
Accepted 10 November 2010
Available online 17 November 2010

Keywords:
Hydrophobically derivatized hyperbranched polyglycerols (HPGs)
Taxanes
Purification
Stability
Cytotoxicity
Cellular uptake

ABSTRACT

In this study we report the development and *in vitro* characterization of paclitaxel (PTX) and docetaxel (DTX) loaded into hydrophobically derivatized hyperbranched polyglycerols (HPGs).

Several HPGs derivatized with hydrophobic groups ($C_{8/10}$ alkyl chains) (HPG–$C_{8/10}$–OH) and/or methoxy polyethylene glycol (MePEG) chains (HPG–$C_{8/10}$–MePEG) were synthesized. PTX or DTX were loaded into these polymers by a solvent evaporation method and the resulting nanoparticle formulations were characterized in terms of size, drug loading, stability, release profiles, cytotoxicity, and cellular uptake.

PTX and DTX were found to be chemically unstable in unpurified HPGs and large fractions (~80%) of the drugs were degraded during the preparation of the formulations. However, both PTX and DTX were found to be chemically stable in purified HPGs. HPGs possessed hydrodynamic radii of less than 10 nm and incorporation of PTX or DTX did not affect their size. The release profiles for both PTX and DTX from HPG–$C_{8/10}$–MePEG nanoparticles were characterized by a continuous controlled release with little or no burst phase of release. *In vitro* cytotoxicity evaluations of PTX and DTX formulations demonstrated a concentration-dependent inhibition of proliferation in KU7 cell line. Cellular uptake studies of rhodamine-labeled HPG (HPG–$C_{8/10}$–$MePEG_{13}$–TMRCA) showed that these nanoparticles were rapidly taken up into cells, and reside in the cytoplasm without entering the nuclear compartment and were highly biocompatible with the KU7 cells.

1. Introduction

Paclitaxel (PTX) and docetaxel (DTX) belong to the taxane family of antimitotic agents and are effective anticancer agents against a wide range of malignancies (Crown and O'Leary, 2000; Pazdur et al., 1993). Their cytotoxic action results from interference with microtubule function in the cell by inhibiting their depolymerization, leading to M-phase cell cycle arrest and cell death (He et al., 2001; Herbst and Khuri, 2003). Given the extremely low water solubility of PTX and DTX (1 and 7 μg/ml, respectively) (Du et al., 2007; Liggins et al., 1997), these agents are formulated in mixtures of surfactants and co-solvents, which have demonstrated some adverse effects including hypersensitivity reactions, nephrotoxicity and neurotoxicity (Gelderblom et al., 2001; ten Tije et al., 2003). Therefore, tremendous effort has focused on the development of alternative and less toxic formulations of PTX and DTX including the use of liposomes (Straubinger and Balasubramanian, 2005), cyclodextrins (Bilensoy et al., 2008), microspheres (Dordunoo et al., 1995), nanoparticles (Gaucher et al., 2010), micelles (Zhang et al., 1997), and polymer-drug conjugates (Li and Wallace, 2008). However, only a few formulations have been successfully applied in clinical settings to date. Opaxio™ (CT-2103, Cell Therapeutics, Inc., Seattle, WA) is a poly(L-glutamic acid)-based PTX conjugate that is currently undergoing clinical trials for the treatment of non-small cell lung, recurrent ovarian and colorectal cancers (Singer, 2005), but has yet to receive an approval. On the other hand, Abraxane® (American BioScience, Inc., Santa Monica, CA), an albumin-bound PTX nanoparticle system (~130 nm) has been approved by the FDA for the treatment of metastatic breast cancer based on Phase III trials, in which Abraxane® showed superior efficacy compared to PTX in Cremophol-EL (Taxol® Bristol-Myers Squibb Co., Princeton, NJ (Sparreboom et al., 2005).

Polymeric micelles based on amphiphilic diblock copolymers of methoxy polyethylene glycol (MePEG) and polyesters have been used successfully to solubilize high payloads of taxanes and other hydrophobic chemotherapeutic agents (Gaucher et al.,

* Corresponding author. Tel.: +1 604 822 2440; fax: +1 604 822 3035.
E-mail address: burt@interchange.ubc.ca (H.M. Burt).

0378-5173/$ – see front matter © 2010 Elsevier B.V. All rights reserved.
doi:10.1016/j.ijpharm.2010.11.010

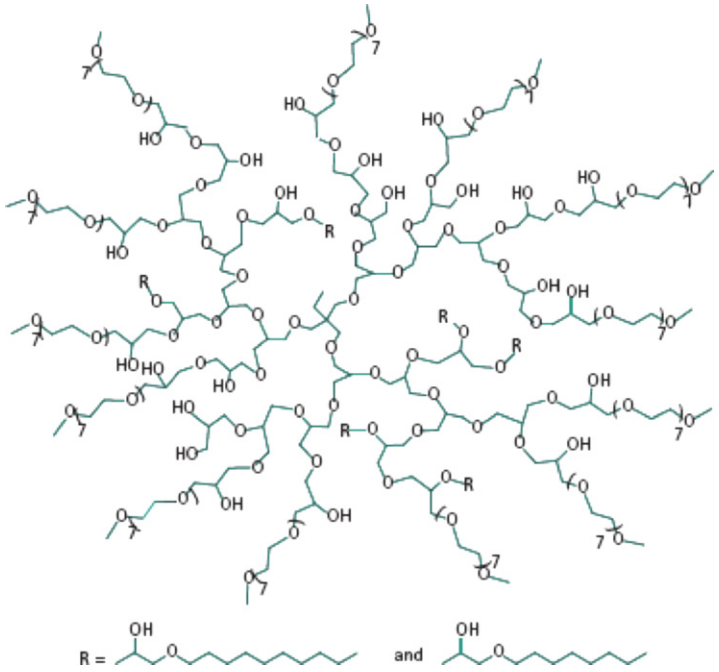

Fig. 1. Structure of HPG–$C_{8/10}$–MePEG. HPG–$C_{8/10}$–OH was derivatized with hydrophobic groups (R, octyl/decyl glycidyl ether) and methoxypolyethylene glycol 350 (MePEG 350) in a single-pot synthetic procedure.

2010; Hadaschik et al., 2008b; Letchford et al., 2008; Leung et al., 2000; Zhang et al., 1997). However, the popularity of these nanoparticulate systems is also related to their pharmacokinetic advantages. They have demonstrated increased circulation lifetime and increased accumulation of entrapped drugs in tumours and inflamed tissues due to the enhanced permeability and retention (EPR) effect (Gaucher et al., 2010; Lee et al., 2010; Zhang et al., 1997). Although, these formulations have shown good *in vitro* physical and chemical stability, following administration and dilution in the blood, micellar formulations are thermodynamically unstable below their critical micelle concentration (CMC). Depending upon the diblock copolymer composition, micelles disassemble below the CMC at different rates (Allen et al., 1999). For example, rapid destabilization of PTX loaded micelles of MePEG-block-poly(DL-lactic acid) caused redistribution of PTX into various plasma components (Ramaswamy et al., 1997).

Brooks and coworkers have developed hyperbranched polymers structurally related to dendrimers that are "unimolecular micelles" and resist dilution effects (Kainthan et al., 2008a,b). Other groups have also reported similar findings (Calderon et al., 2010; Stiriba et al., 2002; Turk et al., 2007; Wilms et al., 2010). These hyperbranched polyglycerols (HPGs) may be hydrophobically derivatized to create a core suitable for loading of hydrophobic drugs (see Fig. 1). MePEG chains conjugated to the outer corona of HPGs provide water solubility and "stealth" characteristics. HPGs possess small hydrodynamic diameters in the range of 3–10 nm and delivery systems in this size range have shown effective accumulation in tumour tissues (Fox et al., 2009; Zhu et al., 2010).

HPGs have been shown to be highly biocompatible and nontoxic both *in vitro* and in animal studies (Kainthan and Brooks, 2007; Kainthan et al., 2007). Following sequential intravenous administrations in mice, these HPGs were found to retain the same circulation half-life as in mice not previously exposed to HPGs so they appear to be non-immunogenic. They also exhibited long circulation half-lives (>30 h) and low organ accumulation owing, in part, to the presence of MePEG chains on the surface of HPGs which protect them against host defenses and from interacting with plasma proteins (Kainthan and Brooks, 2008). Recently, we have reported the encapsulation and subsequent controlled release of PTX from HPGs (Kainthan et al., 2008b). In addition, PTX, incorporated in HPGs, was found to have equivalent cytotoxicities to Taxol® against several bladder cancer cell lines *in vitro*. Furthermore, *in vivo,* PTX loaded HPGs were significantly more effective in reducing orthotopic bladder tumour growth than Taxol® following intravesical administration in a mouse model of bladder cancer (Mugabe et al., 2009).

Although HPGs possess considerable potential as nanoparticulate drug delivery systems, little is known about their physicochemical properties and performance characteristics as drug carriers. The purpose of this study was to characterize hydrophobically derivatized HPGs with varying MePEG contents in terms of purification, drug loading, stability, thermal properties, release profiles, cytotoxicity, and cellular uptake.

2. Materials and methods

2.1. Chemicals

All chemicals were purchased from Sigma-Aldrich (Oakville, ON) and all solvents were HPLC grade from Fisher Scientific (Ottawa, ON). α-epoxy, ω-methoxy polyethylene glycol 350 (MePEG 350 epoxide), was synthesized from a reaction of MePEG 350, sodium hydroxide, and epichlorohydrin. Octyl/decyl glycidyl ether, potassium methylate and trimethyloyl propane (TMP) were obtained from Sigma–Aldrich and used without further purification. Paclitaxel powder was obtained from Polymed Therapeutics, Inc. (Houston, TX) and Taxol® was from Bristol-Myers-Squibb (Princeton, NJ). Docetaxel powder was obtained from Natural Pharmaceuticals Inc. (Beverly, MA) and Taxotere® was purchased from Sanofi-Aventis Canada Inc. (Laval, Quebec). Radioactive drugs (^{3}H-DTX or ^{3}H-PTX) were obtained from Moravek Biochemicals and Radiochemicals (Brea, CA). Dialysis membrane tubing was purchased from Spectrum Laboratories (Rancho Dominguez, CA). Artificial urine was prepared according to the method of Brooks et al. (Brooks and Keevil, 1997), without the addition of peptone or

yeast extract. The pH of the solution was adjusted to pH 4.5 and or 6.5 using 0.1 M HCl.

2.2. Synthesis of hydrophobically modified hyperbranched polyglycerols (HPGs)

2.2.1. Synthesis of HPG–$C_{8/10}$–OH

The polymerizations of octyl/decyl glycidyl ether (O/DGE, $C_{8/10}$) core modified HPGs were carried out according to protocols described earlier by our group (Kainthan et al., 2008b). Briefly, 120 mg of the initiator (TMP) was mixed with 1.5 ml of potassium methylate solution in methanol (25%, w/v) and added to a three-neck round-bottom flask under argon atmosphere. The mixture was stirred at 105 °C for 1 h, after which excess methanol was removed under vacuum, then, 13 ml of glycidol and 9 ml of O/DGE mixture was injected using a syringe pump at a rate of 1.4 ml/h to the initiator. The stirring rate was fixed at 68 rpm using a digital overhead stirring system (BDC2002). After completion of monomer addition the mixture was stirred for an additional 6 h. Purified polymers were obtained by extraction with hexane to remove unreacted octyl/decyl glycidyl ether. The product was then dissolved in methanol and neutralized by passing three times through a cation exchange column (Amberlite IRC-150, Rohm and Haas Co., Philadelphia, PA). Methanol was removed under vacuum and an aqueous solution of the polymer was then dialysed for three days against water using cellulose acetate dialysis tubing (MWCO 10,000 g/mol, Spectrum Laboratories), with three water changes per day.

^{1}H NMR (400 MHz, D_6-DMSO) δ_H: 0.75–0.82 (–C*H*$_3$, TMP); 0.82–0.91 (–C*H*$_3$–alkyl on O/DGE); 1.16–1.53 (–C*H*$_2$–, alkyl on O/DGE); 2.46 (solvent, D_6-DMSO); 3.16–3.80 (–C*H* and –C*H*$_2$–, from HPG core); 4.8 (–O*H*).

2.2.2. Synthesis of HPG–$C_{8/10}$–MePEG

Two batches of HPG–$C_{8/10}$–MePEG were prepared containing different amounts of MePEG and were designated HPG–$C_{8/10}$–$MePEG_{6.5}$ and HPG–$C_{8/10}$–$MePEG_{13}$ to indicate the amount of MePEG added to the feed (6.5 and 13 mol of MePEG per mole of HPG, respectively). The synthesis was carried out in similar fashion as the HPG–$C_{8/10}$–OH reaction except that different amounts of MePEG 350 epoxide were added to the reaction mixture in the final step of the synthesis. Briefly, 120 mg of the initiator (TMP) was mixed with 1.5 ml of potassium methylate solution in methanol (25%, w/v) and added to a three-neck round-bottom flask under argon atmosphere. The mixture was stirred at 105 °C for 1 h, after which excess methanol was removed under vacuum, then, 13 ml of glycidol and 9 ml of O/DGE mixture was injected using a syringe pump at a rate of 1.4 ml/h to the initiator. After all of the mixture of glycidol and O/DGE was injected, the reaction was continued to about 6 h. Then 0.1 ml of potassium hydride (KH) was added to the flask. The mixture was stirred for 1 h, after which 10 ml or 20 ml of MePEG 350 epoxide was added as a terminal step in the "one pot" synthesis using a syringe pump at a rate of 1.4 ml/h. The amount of MePEG 350 was added according to the targeting density on HPGs (i.e 10 ml of MePEG350 is for the targeting of 6.5 mol of MePEG on per mole of HPG). The stirring rate was then increased to 90 rpm and the reaction was continually carried out at 105 °C for overnight. Any traces of unreacted octyl/decyl glycidyl ether were removed by extraction with hexane. The product was dissolved in methanol and neutralized by passing it three times through a cation exchange column (Amberlite IRC-150, Rohm and Haas Co., Philadelphia, PA). Methanol was removed under vacuum and an aqueous solution of the polymer was then dialysed for three days against water using cellulose acetate dialysis tubing (MWCO 10,000 g/mol, Spectrum Laboratories), with three water changes per day. Dry polymer was then obtained by freeze-drying.

^{1}H NMR (400 MHz, D_6-DMSO) δ_H: 0.75–0.82 (–C*H*$_3$, TMP); 0.82–0.92 (–C*H*$_3$–alkyl on O/DGE); 1.15–1.55 (–C*H*$_2$–, alkyl on O/DGE); 2.50 (solvent, D_6-DMSO); 3.15–3.80 (–C*H* and –C*H*$_2$–, from HPG core); 3.23 (–OC*H*$_3$– from MePEG), 3.32 (residual water); 4.8 (–O*H*).

2.3. Characterization of HPGs

The fractions of MePEG and alky chains on HPGs were estimated from heteronuclear single quantum coherence (HSQC) NMR experiments recorded on a Bruker Avance 400 MHz NMR spectrometer using deuterated solvents (Cambridge Isotope Laboratories, 99.8% D). Chemical shifts were referenced to the residual solvent peak. HSQC spectra were analyzed using Sparky (T. D. Goddard and D. G. Kneller, Sparky 3, University of California, San Francisco). Molecular weights and polydispersities of the polymers were determined by gel permeation chromatography with multi-angle laser light scattering detection (GPC-MALLS) as previously reported (Kainthan et al., 2008b).

2.4. Thermal analysis (DSC/TGA) and moisture content

Differential scanning calorimetry (DSC) and thermogravimetric analysis (TGA) were used to evaluate the thermal and degradation properties of the HPGs. Thermal analysis was conducted using a TA Instruments DSC Q100 and a TGA Q50. DSC runs were obtained by cycling weighed samples in hermetic sealed aluminum pans through a "heat-cool-heat" cycle at 10 °C/min over the temperature range of −90 to 85 °C. TGA runs were conducted at a constant ramping temperature program (20.0 °C/min to 500 °C) with a gas flow of 40 ml/min (nitrogen). The real-time weight percentage and TGA chamber temperature were recorded. Analysis of the data was performed using TA Universal Analysis 2000 software (Version 4.2E, TA Instruments) to find the onset points. The amount of water content in HPGs was determined by titration using Mettler Toledo DL39 Karl Fisher Coulometer equipped with AB104-S balance. Known amount of HPGs were dissolved in anhydrous methanol and titrated with HYDRANAL®-Coulomat reagent (Sigma). The final results were obtained by subtracting the background reading from anhydrous methanol.

2.5. Particle size and zeta potential

Particle size and zeta potential analysis was conducted using a Malvern NanoZS Particle Size analyzer using DTS0012 disposable sizing cuvettes for each analysis. Polymer solutions at a concentration of 15 mg/ml were prepared in 1 mM NaCl and filtered with 0.22 μm syringe filter (PALL Acrodisc 13 mm with nylon membrane). Sample acquisition parameters were: angle was 173° back-scatter with automatic attenuation; number of runs 11 (10 s/run); dispersant was water at 25 °C (viscosity 0.8872cP and RI 1.330); Mark-Houwink parameter $A = 0.428$ and $K = 7.67\text{e-}05$ cm^2/s. HPGs were assumed to have a similar refractive index as polyethylene glycol (PEG) with a RI = 1.460 and absorption 0.01. The final data represented the average of all the runs.

2.6. Loading of PTX and DTX into HPGs

PTX or DTX and HPGs were dissolved in 1 ml acetonitrile solution in 4 ml vials and dried in an oven at 60 °C for 1 h and flashed with nitrogen to eliminate traces of the organic solvent. The resulting HPG/taxane matrix was hydrated with 1 ml of 50 °C warm 10 mM phosphate buffered saline (PBS, pH 7.4) and vortexed for 2 min. The resulting solutions were generally clear but in cases where white particles were observed, the solutions were centrifuged

(18,000 × g for 10 min) and supernatants were transferred to new vials.

2.7. Quantification of PTX and DTX

The amount of PTX and DTX incorporated into HPGs was determined by reversed phase HPLC as previously described (Jackson et al., 2004). Briefly, 100 μl of HPG/PTX or DTX solution was dissolved with 900 μl of acetonitrile/water (60:40, v/v) and transferred into HPLC vials (Canadian Life Science, Peterborough, ON). Drug content analysis was performed using a symmetry C18 column (Waters Nova-Pak, Milford, MA) with a mobile phase containing a mixture of acetonitrile, water, and methanol (58:37:5, v/v/v) at a flow rate of 1 ml/min. Sample injection volumes were 20 μl and detection was performed using UV detection at a wavelength of 232 nm. Our HPLC method for quantification of PTX and DTX has been previously validated. This method was evaluated over a linear range of 0.5–100 μg/ml. Over this range, the accuracy (percent deviation from theoretical value) was found to be within 3% and the precision (%RSD) was less than 2% using clean PTX and DTX standards.

2.8. Stability of PTX and DTX in HPGs

The physical and chemical stability of taxane loaded HPGs were evaluated. The physical stability was evaluated by visual observation of clarity of the formulations, where precipitation in less than 24 h was considered a physically unstable formulation. Samples were observed immediately upon rehydration in PBS ($t = 0$), or after 1, 3, 6, 24, 48 and 72 h at room temperature. Chemical stability of PTX and DTX were monitored by the HPLC method as described above. Degradation products were identified by mass spectometry analysis using Waters TQD mass spectrometer. The system was operated at an electrospray ion source block temperature of 150 °C, a desolvation temperature of 350 °C, a cone voltage of 45 kV, a capillary voltage of 0.70 kV, extractor voltage of 3 kV, RF voltage of 0.1 kV, a cone gas flow at 25 l/h, a desolvation gas flow at 600 l/h and a collision gas flow at 0.2 ml/min. The molecules undergo electron spray ionization in the positive ion mode.

2.9. PTX and DTX release from HPGs

PTX and DTX release from HPGs were determined by a dialysis method. Briefly, 100 mg of HPGs (HPG–$C_{8/10}$–$MePEG_{6.5}$ or HPG–$C_{8/10}$–$MePEG_{13}$) were weighed and mixed with 1 mg of PTX or DTX in 1 ml acetonitrile solution, spiked with 15 uCi ^{3}H-DTX or ^{3}H-PTX (15 ul) and dried under nitrogen stream to remove the solvent. The HPGs/taxane matrix was hydrated with 2 ml of PBS and transfered into dialysis bags and dialysed against 500 ml of artificial urine (pH 4.5 or 6.5) with shaking at 100 rpm. At different time points, the volumes of the dialysis bags were measured and a 10 μl sample was taken for measurement of the remaining radioactivity in the dialysis bags and the entire external release media was exchanged with fresh media to maintain sink conditions. The concentration of ^{3}H-DTX or ^{3}H-PTX remaining in the dialysis bag at each time point was determined by beta scintillation counting (Beckman Coulter Canada, Mississagua, ON). The cumulative percent drug released was calculated by substracting the amount of drug remaining at each time point from the initial amount of drug at the beginning of the experiment. The data were expressed as cumulative percentage drug released as a function of time.

2.10. In vitro cytotoxicity studies

The human urothelial carcinoma cell line KU7 was kindly provided by Dr. M. Tachibana (Keio University, Tokyo, Japan). Cells were plated at 5,000 cells/well in 96-well plates in a 100 μl volume of McCoy's Medium supplemented with 10% FBS and allowed to equilibrate for 24 h before freshly prepared solutions of Taxol®, Taxotere®, or PTX or DTX in HPGs (dissolved in PBS, pH 7.4) were added. Cells were exposed to the drugs for 2 h and cell viability was determined after 72 h using the CellTiter96 AQ_{ueous} Non-Radioactive Cell Proliferation Assay (Promega, Madison, WI) as described previously (Hadaschik et al., 2008a). Each experiment was repeated three times and MTS values fell within a linear absorbance range for all cell lines.

2.11. Rhodamine labeling of HPG–$C_{8/10}$–$MePEG_{13}$

HPG–$C_{8/10}$–$MePEG_{13}$ was covalently labeled with tetramethylrhodamine-5-carbonyl azide (TMRCA) according to the method of Huang et al. with slight modifications (Huang et al., 2003). Briefly, 500 mg of HPG–$C_{8/10}$–$MePEG_{13}$ was dissolved in 5 ml of anhydrous 1,4-dioxane. An appropriate amount of TMRCA was dissolved in anhydrous 1,4-dioxane to give a final concentration of 1 mg/ml. An aliquot of 675 μl of this fluorescent probe, which corresponds to approximately 20 mol% of HPG, was added to the HPG–$C_{8/10}$–$MePEG_{13}$ solution and heated at 80 °C in oil bath under nitrogen stream with stirring for 5 h. The solution was dialysed against DMF (MWCO 12,000–14,000) until the dialysate was colourless and then dialysed against distilled water for 24 h. The fluorescent-labeled polymer (HPG–$C_{8/10}$–$MePEG_{13}$–TMRCA) was freeze-dried and stored at −80 °C in amber vials.

2.12. Uptake studies

KU7 cells were allowed to grow on several microscope 1 cm × 1 cm cover slips on the bottom of a 10 cm Petri dish until a confluence of ∼75% was reached which corresponds to a cell number of approximately 7×10^4 cells. These cell-containing cover slips were washed with warmed PBS three times and then placed on parafilm-lined petri dishes with the cell side up. 250 μl of HPG–$C_{8/10}$–$MePEG_{13}$–TMRCA solution (1 mg/ml dissolved in Dulbecco's Modified Eagle Medium (DMEM)) were added to the cover slips. Cells were incubated with HPG–$C_{8/10}$–$MePEG_{13}$–TMRCA for 1, 4, 8, and 24 h. For controls, the KU7 cells were incubated in DMEM without any supplementation. The cover slips were then washed four times vigorously with PBS buffer, excess PBS gently blotted and 250 μl of 3.7% paraformaldehyde added to fix the cells for 10 min. Cover slips were washed an additional three times with PBS and submerged in water. After blotting excess liquid, the cells were stained with Prolong® Gold antifade reagent with DAPI (Molecular Probes, Invitrogen) and the slips mounted cell side down on microscope glass slides. The edges of the cover slips were sealed by clear nail varnish to avoid drying. The samples were incubated in the dark overnight to ensure the proper staining of the cells. Samples were observed under an Olympus FV-1000 inverted confocal microscope equipped with DAPI (λ_{ex} 340–380 nm; λ_{em}, 435–485 nm; dichroic splitter, 400 nm) and rhodamine (λ_{ex} 530–560 nm; λ_{em}, 590–650 nm; dichroic splitter, 570 nm) filters. Direct contrast (DIC) was also performed to visualize cell membranes and was activated with a 405 nm laser. In order to clearly show that the labeled polymer was inside the cell, images were analyzed by fluorescence and DIC.

3. Results

3.1. Synthesis and characterization of HPG–$C_{8/10}$–OH and HPG–$C_{8/10}$–MePEG

Several HPGs derivatized with hydrophobic groups and MePEG chains were synthesized in a single pot synthetic procedure

Table 1
The physical characteristics of HPG–$C_{8/10}$–OH and HPG–$C_{8/10}$–MePEG loaded with PTX and DTX.

HPGs	Structure by NMR (mol/mol HPG)		Molecular weight and polydispersity		Thermal properties			
	MePEG	O/DGE	$M_w \times 10^4$	M_w/M_n	T_g (°C)[a]	T_d (°C)[b]	T_g (PTX)[c]	T_g (DTX)[c]
HPG–$C_{8/10}$–OH	–	4.7	ND	ND	−37.5	338	–	–
HPG–$C_{8/10}$–MePEG$_{6.5}$	4.0	4.7	7.6	1.01	−45.2	341	−68.8	−68.3
HPG–$C_{8/10}$–MePEG$_{13}$	4.6	4.7	8.3	1.22	−55.4	344	−54.9	−58.4

M_w, weight average molecular weight determined by gel permeation chromatography connected to MALLS detector (GPC–MALLS). M_w/M_n polydispersity. ND, not determined.
[a] T_g, glass transition taken at midpoint of transition.
[b] T_d, degradation temperature taken at maximum weight loss.
[c] PTX and DTX were loaded at the maximum loading capacity of HPG–$C_{8/10}$–MePEG.

based on ring-opening polymerization of epoxides. HPG without MePEG chains was designated HPG–$C_{8/10}$–OH and represents the "base polymer" and was prepared by anionic ring opening multibranching polymerization of glycidol from partially deprotonated trimethylol propane (TMP) using potassium methylate. HPG–$C_{8/10}$–OH has numerous terminal hydroxyl end groups, the number per molecule being roughly equal to the degree of polymerization. The HPG–$C_{8/10}$–OH core was derivatized with $C_{8/10}$ alkyl chains to create a hydrophobic core, to allow for the loading of taxanes. Unreacted alkyl epoxides were removed from the methanolic polymer solution by extraction with hexane. HPGs with the targeting densities of 6.5 or 13 mol of MePEG linked to hydroxyl groups in the last phase of the polymerization reaction were designated HPG–$C_{8/10}$–MePEG$_{6.5}$ and HPG–$C_{8/10}$–MePEG$_{13}$, respectively. Since MePEG 350 epoxide was added to the polymerization reaction after reaction of the other components, they create a hydrophilic shell intended to increase the aqueous solubility of these HPGs. However, despite the difference in amount of MePEG added to the reaction feed, there were relatively small differences in the MePEG content between the two batches of HPG–$C_{8/10}$–MePEG (Table 1). Unreacted MePEG epoxides were removed by dialysis. Figs. 2 and 3 are representative proton and 2D HSQC spectra of HPG–$C_{8/10}$–OH and HPG–$C_{8/10}$–MePEG polymers. The HSQC data showed the absence of any unreacted epoxide monomers (Fig. 3), which indicates the absence of any contamination of the polymer by unreacted monomers. Also several overlapping peaks from the 1D NMR spectra such as the CH_3 group of TMP and –CH– and –CH_2– of HPG polymer were resolved in 2D HSQC spectra, which allowed for more detailed characterization of these polymers. By comparing the integrals of the MePEG methoxy-group and the O/DGE methyl group to the integral of the TMP CH_3 group, the fractions of O/DGE and MePEG (mol/mol) was calculated for each HPG polymer. The physicochemical characteristics of HPGs are summarized in Table 1.

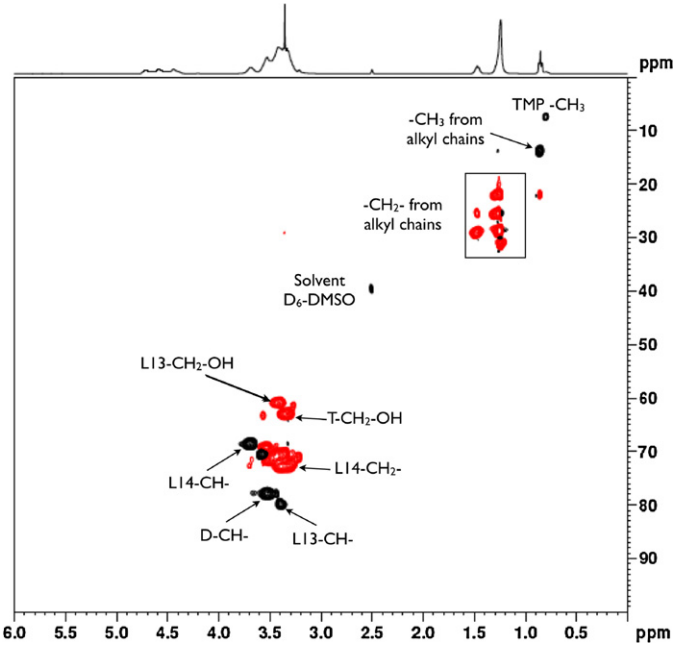

Fig. 2. 400 MHz proton (top) and HSQC spectra of HPG–$C_{8/10}$–OH in D_6-DMSO.

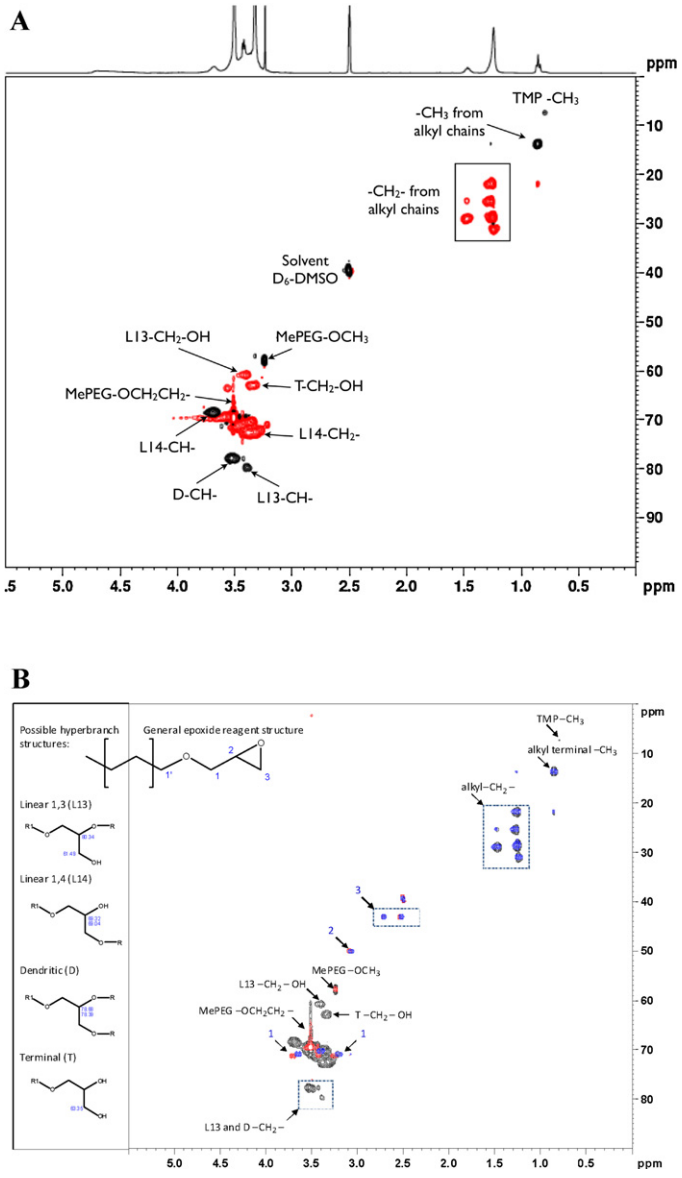

Fig. 3. (A) 400 MHz HSQC proton (top) and HSQC spectra of HPG–$C_{8/10}$–MePEG$_{6.5}$. (B) Superimposed 400 MHz HSQC spectra of MePEG 350 epoxide (red), O/DGE (blue), and HPG–$C_{8/10}$–MePEG$_{13}$ polymer (black). (For interpretation of the references to colour in this figure legend, the reader is referred to the web version of the article.)

Table 2
Effects of polymer purification on polymer properties, and on the physical and chemical stability of taxane loaded formulations made with purified and unpurified HPG–$C_{8/10}$–$MePEG_{13}$.

Polymer properties	Unpurified HPG–$C_{8/10}$–$MePEG_{13}$		Purified HPG–$C_{8/10}$–$MePEG_{13}$	
T_g	−55.8 °C		−55.4 °C	
T_d	310 °C		344 °C	
Water content (%, w/w)	0.326 ± 0.001		2.051 ± 0.001	
pH (10% aqueous solution)	8.5–9		4.4–4.7	
Physical stability (time to precipitation) with increasing taxane loading (%, w/w)[a]	PTX (h)	DTX (h)	PTX (h)	DTX (h)
1.0	>72	>72	>12	>72
2.0	>72	>72	1	>48
3.0	>72	>72	0	24
5.0	>72	>72	0	1
Chemical stability of PTX in "bulk"[b] formulation (% remaining) (t = 0)	26.2		99.8	
Chemical stability of PTX (% remaining) (t = 24 h)	Unpurified		Purified	
In "bulk" matrix	15.6		99.4	
In PBS pH 7.4 constituted formulation	25.8		98.4	

[a] PTX and DTX loading (%, w/w) in HPG–$C_{8/10}$–$MePEG_{13}$, also constituted to an equivalent aqueous concentration (mg/ml).
[b] "Bulk" matrix signifies the taxane loaded HPG–$C_{8/10}$–$MePEG_{13}$ polymer prepared by solvent evaporation prior to constitution with PBS buffer. t = 0 for the bulk matrix is immediately after its final preparation step, drying to remove solvent.

3.2. Effect of purification processes on thermal properties of HPGs

We evaluated the effect of purification processes on the thermal properties of HPGs by DSC and TGA. Purified HPGs are referred to polymers that have been through various purification steps, which involved extraction with hexane to remove unreacted $C_{8/10}$ alkyl chains followed by neutralization through a cation exchange column and then dialysis. HPG–$C_{8/10}$–OH and HPG–$C_{8/10}$–MePEG exhibited glass transitions at temperatures decreasing from −38 to −55 °C as the MePEG content increased from 0 (HPG–$C_{8/10}$–OH) to 4.6 mol MePEG/HPG (Table 1). The purification process had no effect on T_g values of HPGs and there were no significant effects on the thermal stability. Both purified and unpurified HPGs were stable up to a temperature of 300 °C with no indication of thermal decomposition (Table 2).

3.3. Effect of purification processes on physical and chemical stabilities of HPGs loaded PTX and DTX

The effect of purification processes on physical and chemical stabilities of PTX and DTX loaded HPG–$C_{8/10}$–MePEG was also evaluated since there was residual moisture (2.05% by Karl Fischer analysis, Table 2) in the purified polymers due to the dialysis step in the purification procedure which might affect the physical and chemical stabilities of the loaded drugs. Both PTX and DTX were loaded into purified or unpurified HPG–$C_{8/10}$–MePEG and the physical stabilities were evaluated by observing the onset of drug precipitation from PBS (pH 7.4). Chemical stabilities were assessed by LC/MS/MS to determine the amounts of PTX and DTX and their degradation products. The purification processes had significant effects on both the physical and chemical stabilities of PTX and DTX loaded HPGs. Maximum achievable PTX and DTX loadings were greater for unpurified polymers and these formulations were found to be physically more stable than formulations made with purified HPGs (Table 2). Samples prepared with unpurified polymer did not precipitate for several days (>3d), with taxane loading as high as 5% (w/w) whereas those prepared with purified polymer and 5% (w/w) taxane loading precipitated within a few hours, or immediately upon constitution in PBS (Table 2). However, we found that PTX and DTX were chemically unstable in unpurified HPGs and large fractions of the taxanes were degraded during the preparation of the formulations. About 75–80% of PTX was degraded immediately following loading in unpurified HPG–$C_{8/10}$–MePEG regardless of whether it was dry (bulk) matrix or after it was reconstituted in PBS (pH 7.4) (Table 2). However, once in buffer no further PTX degradation occurred, whereas PTX in the dry matrix continued to degrade over 24 h. Fig. 4B shows a chromatogram from a formulation of PTX in unpurified HPG-$C_{8/10}$-MePEG, with a peak corresponding to PTX and other peaks resulting from the formation of several degradation products. The chromatogram was obtained from a formulation dissolved in acetonitrile immediately after solvent drying (e.g. in the bulk state, prior to constitution in PBS). Two major degradants were identified by LC/MS/MS, having m/z values of 587 and 854, respectively. Based on these masses and the relative retention times of these peaks, their identities are assumed to be baccatin III (m/z 587, Fig. 4A) and 7-epi-taxol (m/z 854), respectively; however standards of these degradants were not available for confirmation. Other degradation products (peak A & B, Fig. 4B) were also observed in unpurified formulations. Taxanes loaded in purified polymers however, exhibited quite different behavior. PTX was found to be chemically stable both in bulk and in solution for several days and no major degradants were observed during the preparation of the formulations (Table 2 and Fig. 5C).

3.4. PTX and DTX loading in HPGs

Increased MePEG content in HPGs resulted in decreases in T_g from −38 to −55 °C and loading with PTX or DTX also decreased the T_g (Table 1). HPG–$C_{8/10}$–OH had a limited aqueous solubility resulting in low drug loading of taxanes (data not shown). A relatively small increase in the amount of MePEG in the HPGs resulted in increased drug loading of HPG–$C_{8/10}$–$MePEG_{13}$ for both PTX and DTX. However, the maximum loading of DTX (5%, w/w) was greater than for PTX in HPG–$C_{8/10}$–$MePEG_{13}$ (2%, w/w). HPG particles sizes were consistently less than 10 nm in diameter with the loading of PTX and DTX having no effect on the size of HPG–MePEG (data not shown).

3.5. PTX and DTX release profiles

The release of PTX and DTX from HPG–$C_{8/10}$–$MePEG_{13}$ into artificial urine was evaluated since we are developing these formulations for intravesical administration in bladder cancer. The pH of urine is acidic but is known to vary over a wide range (pH 4.5–8), therefore we evaluated the effect of pH on the release profiles PTX and DTX loaded in HPG–$C_{8/10}$–MePEG. The release studies were performed using the dialysis method and sink conditions were maintained by regularly replacing the dialysis medium. The release profiles for both PTX and DTX from HPG–$C_{8/10}$–MePEG

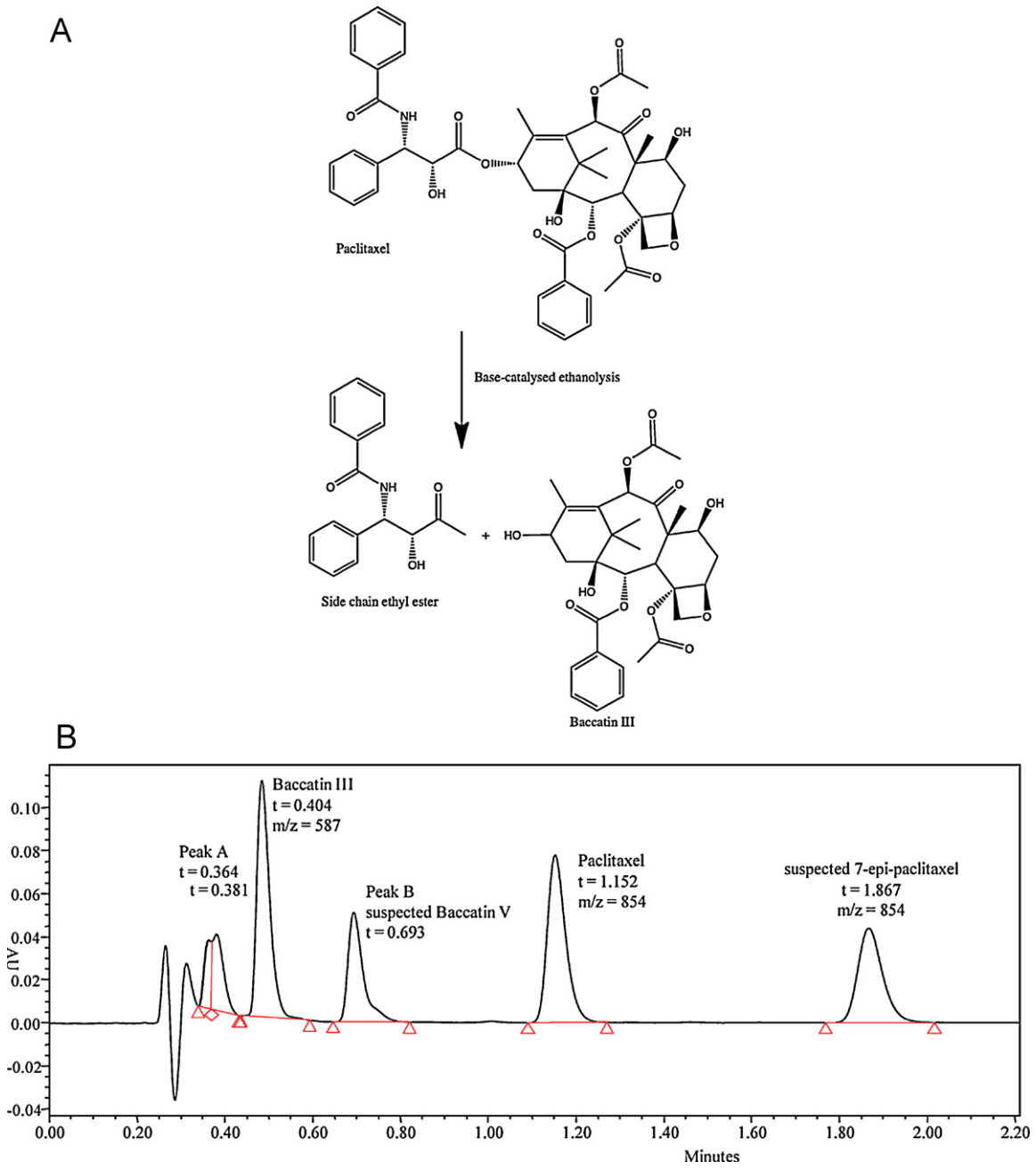

Fig. 4. (A) Base-catalyzed ethanolysis of PTX ester linkage to generate Baccatin III and its side chain ethyl ester (N-benzoyl-3-phenylisoserine ethyl ester). (B) Representative chromatograms illustrating the identification of degradants of PTX by a UPLC–MS/MS assay in a formulation prepared using unpurified HPG–$C_{8/10}$–MePEG. The sample is from the "bulk" formulation, prior to constitution with PBS.

were characterized by a continuous controlled release with little or no burst phase of release (Fig. 6). However, DTX was released more rapidly than PTX (75% vs 50% drug release after 2 days) from HPG–$C_{8/10}$–MePEG. Increases in the density of MePEG on HPGs had no effect on drug release (Fig. 6A). Similarly changes in the pH of the release medium (pH 4.5–6.5) had no effect on drug release from HPG–$C_{8/10}$–MePEG nanoparticles (Fig. 6B). Evaluation of release profiles of PTX and DTX from the HPG nanoparticles using various kinetic models (including first order, higuchi, and korsmeyer model) indicated that both the first order and the higuchi kinetics provided the best fit with r^2 = 0.98–0.99 (data not shown). There was no statistical difference between the formulations in terms of rate of drug release (data not shown).

3.6. *In vitro cytotoxicity of PTX and DTX in HPG–$C_{8/10}$–MePEG*

We evaluated the cytotoxic effects of commercial formulations, Taxol® and Taxotere® and PTX and DTX loaded HPG–$C_{8/10}$–MePEG formulations against a human urothelial carcinoma cell line, KU7. Cells were exposed to the drug formulations for 2 h, to simulate the current clinical standard for instillation therapy, and cell viability was determined after 72 h by MTS assay (Fig. 7). All formulations resulted in concentration-dependent inhibition of the proliferation of KU7 cells. However, DTX formulations were more cytotoxic than PTX formulations, although, there was no significant difference between groups ($P > 0.05$, One-way ANOVA). The IC_{50} of Taxotere® was about two and half fold lower than that of

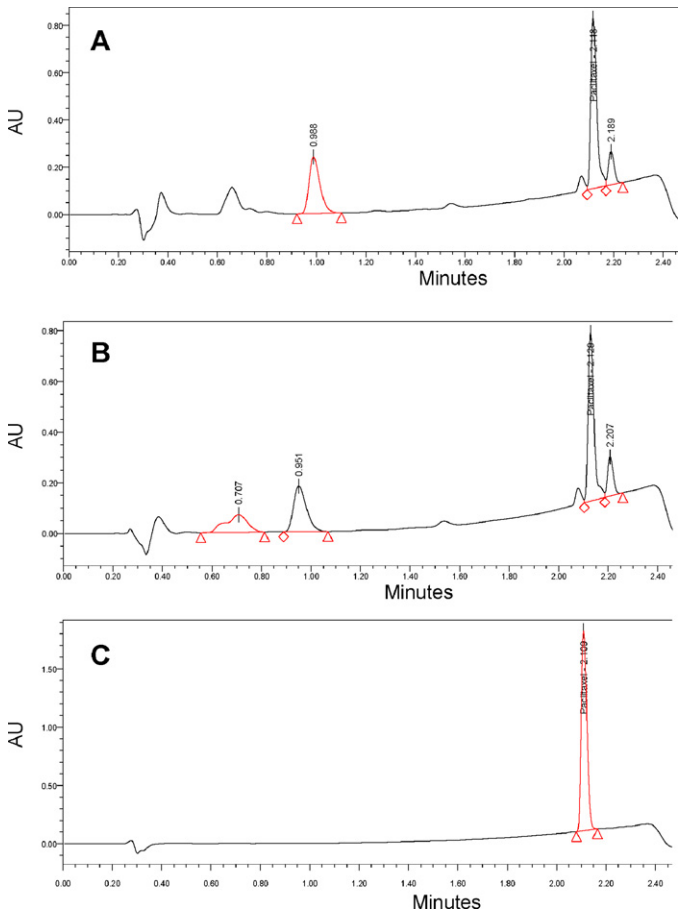

Fig. 5. Representative chromatograms illustrating the effect of purification of HPG–$C_{8/10}$–$MePEG_{13}$ on the chemical stability of PTX (retention time of 2.1 min) measured by UPLC UV analysis. (A) Chromatogram of PTX formulated into unpurified HPG freshly constituted in PBS (pH 7.4), (B) a chromatogram of the same formulation in (A), aged 48 h, and (C) a chromatogram of PTX formulated into purified HPG, freshly constituted in PBS (pH 7.4).

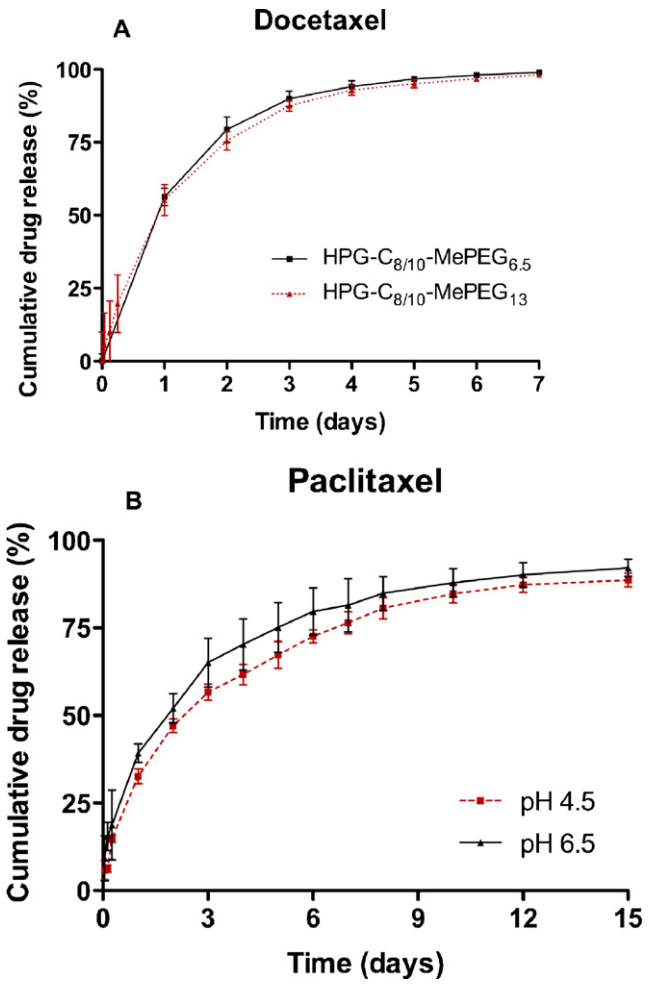

Fig. 6. PTX and DTX release from HPG–$C_{8/10}$–MePEG in artificial urine at 37 °C. (A) Cumulative DTX release from HPG–$C_{8/10}$–MePEG (6 and 13 mol). (B) Cumulative PTX release from HPG–$C_{8/10}$–MePEG in artificial urine (pH 4.6 and 6.5). Data represent the mean (SD) of three independent experiments. Note the difference in scale in the x-axes when comparing A and B.

Taxol® (4 vs 10 nM). PTX and DTX loaded HPG–$C_{8/10}$–MePEG were found to be as cytotoxic as the commercial formulations except for the HPG–$C_{8/10}$–$MePEG_{6.5}$ loaded DTX which was slightly less cytotoxic than Taxotere®. Control HPG–$C_{8/10}$–MePEG nanoparticles (no drug) showed no cytotoxicity across the concentration range of 15–1500 nM (data not shown).

3.7. Cellular uptake of rhodamine-labeled HPG–$C_{8/10}$–$MePEG_{13}$

Confocal microscopy of KU7 cells that were incubated with rhodamine-labeled HPG–$C_{8/10}$–$MePEG_{13}$ (HPG–$C_{8/10}$–$MePEG_{13}$–TMRCA) allows for the visualization of cellular uptake of the polymer. After one hour incubation there was strong evidence of the uptake of HPG–$C_{8/10}$–$MePEG_{13}$–TMRCA into KU7 cells. Representative images of the uptake of HPG–$C_{8/10}$–$MePEG_{13}$–TMRCA at 1 h are shown in Fig. 8. The presence of HPG-$C_{8/10}$–$MePEG_{13}$–TMRCA in the cytoplasm is shown by the red fluorescence of the polymer around the nucleus (stained blue with DAPI). This uptake was confirmed by the z-stack images (Fig. 8C), which showed the presence of the HPG–$C_{8/10}$–$MePEG_{13}$–TMRCA nanoparticles throughout the cytoplasm rather than being only adhered to or present in cell membrane. There was no fluorescence from the polymer detected in the nuclear compartment of the KU7 cells. HPG–$C_{8/10}$–$MePEG_{13}$–TMRCA nanoparticles have no effect on the viability and prevalence of the KU7 cells when compared to the control cells at all time points. Overall, HPG–$C_{8/10}$–$MePEG_{13}$–TMRCA nanoparticles were taken up into KU7 cells by 1 h of incubation and there were no differences in the images obtained at 1, 4, 8 or 24 h time points.

4. Discussion

In this study we have reported the development of nanoparticulate formulations of PTX and DTX based on HPGs. HPGs derivatized with hydrophobic groups within the core and varying amounts of MePEG chains incorporated in the polymer (presumably on the surface) were synthesized in a simple one pot synthetic procedure based on anionic ring-opening multibranching polymerization of epoxides. First the initiator trimethylol propane (TMP) was activated by potassium methylate and reacted with glycidol and octyl/decyl glycidyl ether to create an HPG–$C_{8/10}$–OH with a hydrophobic core to allow the loading of PTX and DTX. To increase the aqueous solubility of HPGs, MePEG 350 epoxide was added in the terminal phase of the reaction, resulting in MePEG 350 chains being linked to some of the hydroxyl groups on HPG to form a more hydrophilic shell, relative to HPG–$C_{8/10}$–OH.

A series of NMR experiments were conducted to characterize the structure of the HPG polymers. All the peaks were assigned to the structural components of the HPGs, using the raw material spectra as the starting reference (Fig. 3B). The proton NMR spectra

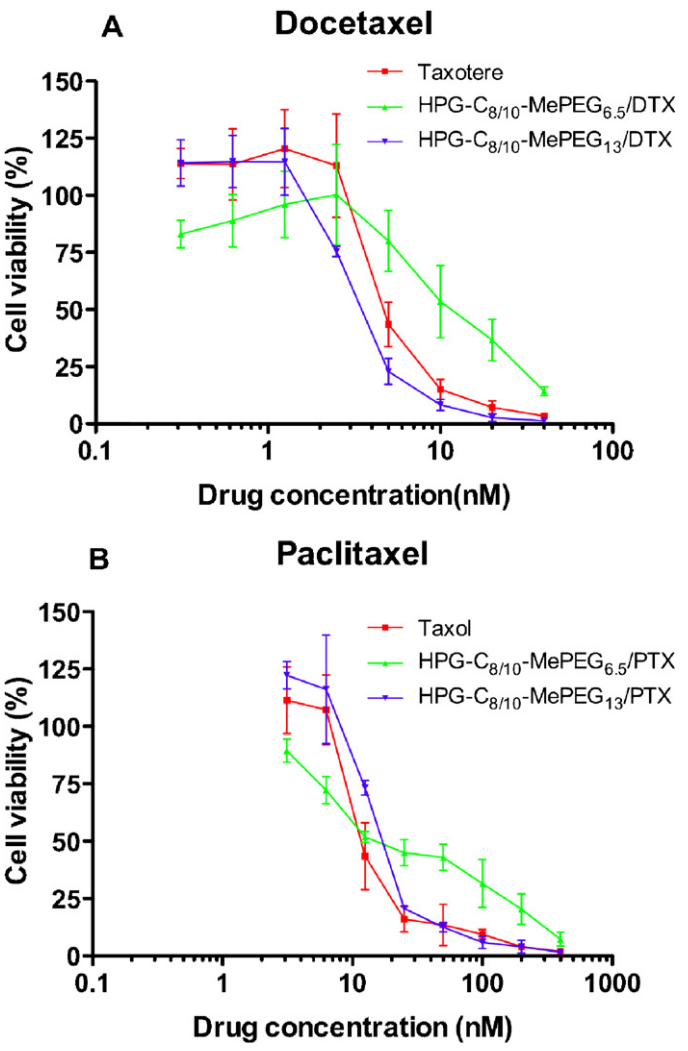

Fig. 7. *In vitro* cytotoxicity of PTX and DTX loaded HPG–$C_{8/10}$–MePEG on KU7. Cells were exposed to PTX and DTX formulations for 2 h and cell viability was determined after 72 h using the CellTiter96 AQ_{ueous} Non-Radioactive Cell Proliferation Assay.

were similar to those previously reported by our group (Kainthan et al., 2008a,b). However, the 2D HSQC spectra for these HPGs have not been reported to date. HSQC NMR data confirmed the structure of HPGs as hyperbranched polymers with the branching architectures evident in the spectra (Figs. 2 and 3). The fractions of each of the substituents can be calculated from the volume integrals in HSQC experiments. This method is considered to be more accurate than the calculations from the 1D NMR spectra as a number of overlapping peaks can be resolved e.g. the CH_3 group of TMP. By comparing the integrals of the MePEG methoxy-group and the O/DGE methyl group to the integral of the TMP CH_3 group, the fractions of O/DGE and MePEG (mol/mol) were calculated for each HPG polymer. Molecular weights were around 80,000 g/mol (Table 1).

We evaluated the effect of the purification process on the physicochemical characteristics of PTX and DTX loaded HPGs since the moisture in the purified polymer resulting from the dialysis step in the purification procedure might affect the physical or chemical stability of the loaded taxane. Indeed, the purification process had significant effects on drug loading, chemical and physical stability of PTX and DTX loaded HPGs. The physical stability and maximum drug loading levels were greater in unpurified HPGs than purified HPGs. Based on these observations, it was first hypothesized that the purification process may have removed a critical component of HPGs (i.e. $C_{8/10}$ alkyl chains) that solubilized the drugs. Alternatively, an increase in water content in the polymer due to dialysis during purification could have resulted in both reduced drug loading capacity and physical stability of the purified polymers. However, in the subsequent experiments, we showed that PTX and DTX loaded in unpurified HPGs underwent extensive drug degradation even prior to constitution in PBS (Fig. 4B). The major degradation products were identified by LC/MS/MS to be baccatin III and 7-epi-taxol, although some other unknown degradation products were also observed in unpurified HPGs. Based on their relative retention times, peak areas, and the known degradation mechanisms of taxanes, peak B (Fig. 4B) is believed to be baccatin V, which is the 7-epi-baccatin III, while peak A is believed to be 10-deacetylbaccatin III. PTX and DTX have four hydrolysable ester groups that might be expected to undergo hydrolysis. Tian and Stella (Tian and Stella, 2008b) have shown that the degradation of taxanes under neutral to basic conditions is a base catalyzed hydrolysis of their ester groups. Under neutral and basic conditions in aqueous solution, taxanes undergo epimerization at C7 (7-epi-taxanes) followed by hydrolysis of the side chain cleavage,

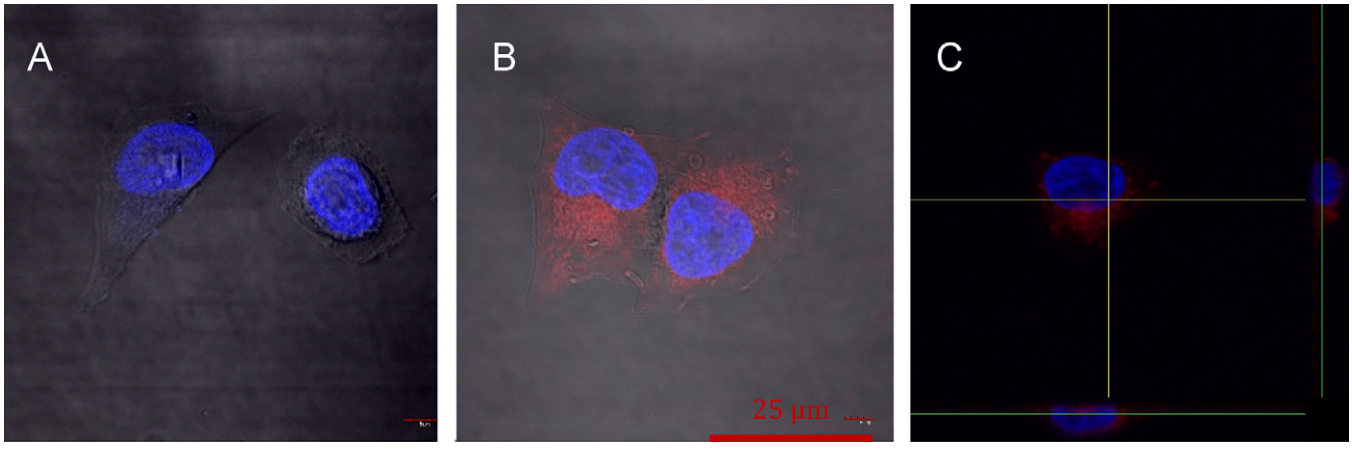

Fig. 8. Confocal fluorescence imaging of KU7 cells illustrating complete uptake of HPG–$C_{8/10}$–$MePEG_{13}$–TMRCA nanoparticles after a 1 h exposure. Panel A shows untreated KU7 cells with a DAPI stain, which allows visualization of the nuclei in blue. The image is an overlay of a direct contrast signal (which shows the contour of the cell) and the fluorescence signals, which shows the nucleus (blue), and the absence of any other (red) fluorescence. Panel B shows KU7 cells that have been incubated for 1 h with HPG–$C_{8/10}$–$MePEG_{13}$–TMRCA nanoparticles. Panel C shows a z-stack of the same cell population from panel B, demonstrating that the red fluorescent nanoparticles are present throughout the cytoplasm, rather than being only adhered to or present in cell membrane. (For interpretation of the references to colour in this figure legend, the reader is referred to the web version of the article.)

yielding baccatin III and baccatin V for PTX (or 10-deactylated baccatins for DTX) with further hydrolysis of the other ester bonds (Tian and Stella, 2008a, b). Our data show that PTX and DTX in unpurified HPGs are quickly degraded and this is probably due to the presence of basic impurities in the unpurified polymers. The most likely basic impurities came from the excess of potassium methylate and potassium hydride added during the synthesis of HPGs. Both potassium methylate and hydride are strong bases and in combination with the residual moisture in the polymer would create an environment favorable for both epimerization at the C7 position and ester cleavage of PTX to produce baccatin III (or 10-deacetyl baccatin III for DTX) (Fig. 4A). The measurement of the pH of HPG polymers in distilled water showed that unpurified polymers had a basic pH while purified polymers had an acidic pH (due to the treatment with Amberlite IRC-150, a cation exchange resin), a more stable environment for taxanes. Previous work from our lab and the recent work by Tian and Stella have shown the maximum stability of taxanes to be in the pH range of 3–5 (Dordunoo and Burt, 1996; Tian and Stella, 2010). The purified polymers were within this pH range (Table 2), hence the improved chemical stability of the loaded taxanes. Based on these observations, it is evident that appropriate purification processes for the polymer is a critical step in the production of chemically stable taxane formulations. Recently, Gogate et al. (2009) have shown the importance of purification of Cremophor-EL® on the stability of Taxol®. They studied the effect of unpurified Cremophor-EL® on the solution stability of PTX and found that the carboxylate anions present in unpurified Cremophor-EL® significantly degraded PTX during storage (Gogate et al., 2009). The apparent higher drug loadings and greater physical stability of taxanes loaded in unpurified HPG polymers may be explained by the fact that majority of the loaded drugs were degraded to smaller and more hydrophilic molecules (baccatin III and baccatin V) than the parent taxanes, suggesting that these degraded molecules were more effectively loaded into HPGs.

The effect of MePEG derivatization on thermal properties, surface charge and drug loading of HPGs was also studied. The presence of MePEG chains on the surface of HPGs had no significant effect on the overall surface charge on these nanoparticles as measured by the zeta potentials as follows: HPG–$C_{8/10}$–OH = -1.29 ± 0.97 mV; HPG–$C_{8/10}$–$MePEG_{6.5}$ = -0.92 ± 1.68 mV; HPG–$C_{8/10}$–$MePEG_{13}$ = 0.18 ± 0.16 mV. On the other hand we found significant effects on the glass transition temperature with increasing MePEG density. The T_g decreased from $-37.5\,^{\circ}C$ for the HPG–$C_{8/10}$–OH polymer to -45.2 and $-55.4\,^{\circ}C$ for the HPG–$C_{8/10}$–$MePEG_{6.5}$ and HPG–$C_{8/10}$–$MePEG_{13}$, respectively (Table 1). Unlike linear polymers, HPGs do not demonstrate chain entanglements within the nanoparticle bulk; the thermal behavior of these hyperbranched polymers is mainly dominated by the intramolecular effects. The HPGs in these studies had approximately eight generations of branching so the contribution of the outer layers to the entire molecular flexibility is considerably higher than the interior, that is mostly restricted (Stutz, 1995). Therefore, the presence of MePEG chains on the surface of HPGs is expected to decrease the T_g due to high molecular flexibility of the MePEG chains. The drug loading for HPG–$C_{8/10}$–OH polymer was very low and this was probably due to the low water solubility of this polymer. The presence of alkyl ($C_{8/10}$) chains in HPGs is important for loading of hydrophobic drugs, however it also significantly reduces their water solubility. To increase the water solubility of HPGs, MePEG 350 chains were added in the terminal phase of the reaction during the synthesis these molecules. The presence of the MePEG chains resulted in increased drug loading of PTX and DTX. This is in agreement with previous reports (Bhadra et al., 2003; Kontoyianni et al., 2008; Tziveleka et al., 2006) suggesting that the presence of MePEG chains enhances the solubilization efficiency of these dendritric-like polymers. Tziveleka et al. (Tziveleka et al., 2006) have reported increased loadings of both pyrene (hydrophobic probe) and tamoxifen (hydrophobic anticancer drug) in hyperbranched polyether polyols derivatized with MePEG chains compared to the unmodified polymers. DTX loading in HPGs was higher than for PTX and this is probably due to the fact that DTX is a slightly smaller and more hydrophilic molecule than PTX, as previously noted. HPGs loaded with DTX showed greater physical stability than PTX formulations. Our data are in agreement with previous work with micelles composed of MePEG750-*b*-oligo(€-caprolactone)$_5$ in which the DTX exhibited higher drug loading and more stable micellar formulations than PTX (Carstens et al., 2008).

The release profiles of taxanes from HPGs were characterized by a continuous controlled release and little or no burst phase of release followed by a slower sustained-release phase, similar to previous release data for PTX loaded HPGs (Kainthan et al., 2008b; Mugabe et al., 2009). DTX was released from HPGs faster than for PTX, with almost all DTX released in 6–7 days, compared to 12–14 days for PTX. This was likely due to the greater hydrophilicity of DTX. There is extensive literature demonstrating that hydrophilic drugs are released more rapidly from polymer matrices as water penetrates the polymer matrix (Rosenberg et al., 2007; Sheikh et al., 2009; Zhang et al., 2007). In addition, the degree of compatibility between the drug and the nature of the core is known to affect the release rate of the encapsulated drug (Letchford and Burt, 2007). Therefore, the more hydrophobic PTX may have greater compatibility and interactions with the alkyl chains (C_8/C_{10}) of the HPG core leading to a slower drug release rate.

In vitro cytotoxicity evaluations of PTX and DTX formulations demonstrated a concentration-dependent inhibition of proliferation in KU7 cell line. PTX and DTX loaded HPGs were found to be as cytotoxic as their counterpart commercial formulations except for the HPG–$C_{8/10}$–$MePEG_{6.5}$ loaded DTX which was slightly less cytotoxic than Taxotere®. Our previous work also showed that PTX loaded HPGs had similar cytotoxicity to Taxol® against several bladder cancer cell lines (Mugabe et al., 2009). However, DTX formulations were more cytotoxic than PTX formulations, as has been previously reported. Otava et al. (Otova et al., 2006) showed a three-fold higher cytoxocity of DTX against P388D1 murine leukemia cell line than PTX. Many other studies have shown DTX to be more potent than PTX both in cell cultures and in animal models (Grant et al., 2003; Rangel et al., 1994; Tanaka et al., 1996; Verweij et al., 1994; Zoli et al., 1995). The increased cytotoxicity of DTX is thought to be due to its higher binding affinity (~2 fold) to microtubules than PTX (Diaz et al., 1998; Gaucher et al., 2010). Control HPG–$C_{8/10}$–MePEG nanoparticles (no drug) showed no evidence of toxicity across the tested concentration range, while Cremophor-EL® and Tween 80 have been shown to be toxic to cells even at low concentrations (Henni-Silhadi et al., 2007; Iwase et al., 2004).

Cellular uptake studies of rhodamine-labeled HPG–$C_{8/10}$–$MePEG_{13}$ (HPG–$C_{8/10}$–$MePEG_{13}$–TMRCA) showed that these nanoparticles were rapidly taken up into the KU7 cells. The fluorescence from HPG–$C_{8/10}$–$MePEG_{13}$–TMRCA nanoparticles was detected in the cytoplasmic but not the nuclear compartment of KU7 cells (Fig. 8). These nanoparticles appeared to be distributed uniformly in the cytoplasm, although some punctate structures were observed indicating that HPG–$C_{8/10}$–$MePEG_{13}$–TMRCA nanoparticles were packaged into small vesicles for cellular trafficking. HPG–$C_{8/10}$–$MePEG_{13}$–TMRCA nanoparticles appeared to have no effect on the viability of the KU7 cells when compared to the control cells, indicating that these nanoparticles were highly biocompatible with this cell line. The mechanism by which the HPGs were internalized by cells was not investigated in this work. However, many nanoparticles including liposomes, micelles, dendrimers and quantum dots have been shown to be internalized

by cells via pino- or endo-cytosis mechanisms (Kunzmann et al., 2010; Qi et al., 2009; Savic et al., 2003).

5. Conclusion

In this study, we report the preparation and characterization of PTX and DTX nanoparticulate formulations based on hydrophobically derivatized hyperbranched polyglycerols (HPGs). The critical importance of appropriate purification procedures for HPGs was demonstrated, since the presence of basic impurities dramatically decreased chemical stability of loaded taxanes. HPGs loaded with DTX were physically more stable with higher drug loading than PTX formulations. *In vitro* cytotoxicity evaluations of PTX and DTX formulations demonstrated a concentration-dependent inhibition of proliferation in KU7 cell line. In general, PTX and DTX loaded HPGs were found to be as cytotoxic as their counterpart commercial formulations. However, DTX formulations were more potent than PTX formulations. Cellular uptake studies of rhodamine-labeled HPG-$C_{8/10}$-MePEG$_{13}$ showed that these nanoparticles were rapidly taken up into KU7 cells, and reside in the cytoplasm of the cells without entering the nuclear compartment and were highly biocompatible with the KU7 cells.

Drug loaded HPGs form extremely small nanoparticles of less than 10 nm, making them substantially smaller than other polymeric nanoparticles, including micelles, nanospheres, nanocapsules and polymersomes (Letchford and Burt, 2007). Furthermore, HPGs are stable unimolecular structures and cannot disassemble upon dilution, offering a nanoparticulate formulation with different properties over other amphiphilic diblock copolymer micelle formulations.

Acknowledgements

We would like to thank Lindsay Heller for her excellent help with the cellular uptake studies. The above work was supported by an operating grant from the Canadian Institutes of Health Research (H.M.B. and D.E.B.), the Natural Sciences and Engineering Research Council of Canada and Michael Smith Foundation for Health Research (C.M. and D.E.B), Canadian Blood Services (D.E.B.). Research performed with the assistance of the LMB Macromolecular Hub at the Centre for Blood Research was supported in part by grants from the Canada Foundation for Innovation and the Michael Smith Foundation for Health Research. This work was also supported with support from the Centre for Drug Research and Development and a grant from the Canada Foundation for Innovation (CFI).

References

Allen, C., Maysinger, D., Eisenberg, A., 1999. Nano-engineering block copolymer aggregates for drug delivery. Colloid Surf. B 16, 3–27.
Bhadra, D., Bhadra, S., Jain, S., Jain, N.K., 2003. A PEGylated dendritic nanoparticulate carrier of fluorouracil. Int. J. Pharm. 257, 111–124.
Bilensoy, E., Gurkaynak, O., Ertan, M., Sen, M., Hincal, A.A., 2008. Development of non-surfactant cyclodextrin nanoparticles loaded with anticancer drug paclitaxel. J. Pharm. Sci. 97, 1519–1529.
Brooks, T., Keevil, C.W., 1997. A simple artificial urine for the growth of urinary pathogens. Lett. Appl. Microbiol. 24, 203–206.
Calderon, M., Quadir, M.A., Sharma, S.K., Haag, R., 2010. Dendritic polyglycerols for biomedical applications. Adv. Mater. 22, 190–218.
Carstens, M.G., de Jong, P.H., van Nostrum, C.F., Kemmink, J., Verrijk, R., de Leede, L.G., Crommelin, D.J., Hennink, W.E., 2008. The effect of core composition in biodegradable oligomeric micelles as taxane formulations. Eur. J. Pharm. Biopharm. 68, 596–606.
Crown, J., O'Leary, M., 2000. The taxanes: an update. Lancet 355, 1176–1178.
Diaz, J.F., Valpuesta, J.M., Chacon, P., Diakun, G., Andreu, J.M., 1998. Changes in microtubule protofilament number induced by Taxol binding to an easily accessible site. Internal microtubule dynamics. J. Biol. Chem. 273, 33803–33810.
Dordunoo, S.K., Burt, H.M., 1996. Solubility and stability of taxol: effects of buffers and cyclodextrins. Int. J. Pharm. 133, 191–201.
Dordunoo, S.K., Jackson, J.K., Arsenault, L.A., Oktaba, A.M., Hunter, W.L., Burt, H.M., 1995. Taxol encapsulation in poly(epsilon-caprolactone) microspheres. Cancer Chemother. Pharmacol. 36, 279–282.
Du, W., Hong, L., Yao, T., Yang, X., He, Q., Yang, B., Hu, Y., 2007. Synthesis and evaluation of water-soluble docetaxel prodrugs-docetaxel esters of malic acid. Bioorg. Med. Chem. 15, 6323–6330.
Fox, M.E., Guillaudeu, S., Frechet, J.M., Jerger, K., Macaraeg, N., Szoka, F.C., 2009. Synthesis and in vivo antitumor efficacy of PEGylated poly(L-lysine) dendrimer-camptothecin conjugates. Mol. Pharm. 6, 1562–1572.
Gaucher, G., Marchessault, R.H., Leroux, J.C., 2010. Polyester-based micelles and nanoparticles for the parenteral delivery of taxanes. J. Control. Release 143, 2–12.
Gelderblom, H., Verweij, J., Nooter, K., Sparreboom, A., 2001. Cremophor EL: the drawbacks and advantages of vehicle selection for drug formulation. Eur. J. Cancer 37, 1590–1598.
Gogate, U.S., Schwartz, P.A., Agharkar, S.N., 2009. Effect of unpurified Cremophor EL on the solution stability of paclitaxel. Pharm. Dev. Technol. 14, 1–8.
Grant, D.S., Williams, T.L., Zahaczewsky, M., Dicker, A.P., 2003. Comparison of antiangiogenic activities using paclitaxel (taxol) and docetaxel (taxotere). Int. J. Cancer 104, 121–129.
Hadaschik, B.A., Adomat, H., Fazli, L., Fraet, Y., Andersen, R.J., Gleave, M.E., So, A.I., 2008a. Intravesical chemotherapy of high grade bladder cancer with HTI-286, a synthetic analogue of the marine sponge product hemiasterlin. Clin. Cancer Res. 14, 1510–1518.
Hadaschik, B.A., ter Borg, M.G., Jackson, J., Sowery, R.D., So, A.I., Burt, H.M., Gleave, M.E., 2008b. Paclitaxel and cisplatin as intravesical agents against non-muscle-invasive bladder cancer. BJU Int. 101, 1347–1355.
He, L., Orr, G.A., Horwitz, S.B., 2001. Novel molecules that interact with microtubules and have functional activity similar to Taxol. Drug Discov. Today 6, 1153–1164.
Henni-Silhadi, W., Deyme, M., Boissonnade, M.M., Appel, M., Le Cerf, D., Picton, L., Rosilio, V., 2007. Enhancement of the solubility and efficacy of poorly water-soluble drugs by hydrophobically-modified polysaccharide derivatives. Pharm. Res. 24, 2317–2326.
Herbst, R.S., Khuri, F.R., 2003. Mode of action of docetaxel—a basis for combination with novel anticancer agents. Cancer Treat Rev. 29, 407–415.
Huang, S.N., Phelps, M.A., Swaan, P.W., 2003. Involvement of endocytic organelles in the subcellular trafficking and localization of riboflavin. J. Pharmacol. Exp. Ther. 306, 681–687.
Iwase, K., Oyama, Y., Tatsuishi, T., Yamaguchi, J.Y., Nishimura, Y., Kanada, A., Kobayashi, M., Maemura, Y., Ishida, S., Okano, Y., 2004. Cremophor EL augments the cytotoxicity of hydrogen peroxide in lymphocytes dissociated from rat thymus glands. Toxicol. Lett. 154, 143–148.
Jackson, J.K., Smith, J., Letchford, K., Babiuk, K.A., Machan, L., Signore, P., Hunter, W.L., Wang, K., Burt, H.M., 2004. Characterization of perivascular poly(lactic-co-glycolic acid) films containing paclitaxel. Int. J. Pharma. 283, 97–109.
Kainthan, R.K., Brooks, D.E., 2007. In vivo biological evaluation of high molecular weight hyperbranched polyglycerols. Biomaterials 28, 4779–4787.
Kainthan, R.K., Brooks, D.E., 2008. Unimolecular micelles based on hydrophobically derivatized hyperbranched polyglycerols: biodistribution studies. Bioconjug. Chem. 19, 2231–2238.
Kainthan, R.K., Hester, S.R., Levin, E., Devine, D.V., Brooks, D.E., 2007. In vitro biological evaluation of high molecular weight hyperbranched polyglycerols. Biomaterials 28, 4581–4590.
Kainthan, R.K., Janzen, J., Kizhakkedathu, J.N., Devine, D.V., Brooks, D.E., 2008a. Hydrophobically derivatized hyperbranched polyglycerol as a human serum albumin substitute. Biomaterials 29, 1693–1704.
Kainthan, R.K., Mugabe, C., Burt, H.M., Brooks, D.E., 2008b. Unimolecular micelles based on hydrophobically derivatized hyperbranched polyglycerols: ligand binding properties. Biomacromolecules 9, 886–895.
Kontoyianni, C., Sideratou, Z., Theodossiou, T., Tziveleka, L.A., Tsiourvas, D., Paleos, C.M., 2008. A novel micellar PEGylated hyperbranched polyester as a prospective drug delivery system for paclitaxel. Macromol. Biosci. 8, 871–881.
Kunzmann, A., Andersson, B., Thurnherr, T., Krug, H., Scheynius, A., Fadeel, B., 2010. Toxicology of engineered nanomaterials: Focus on biocompatibility, biodistribution and biodegradation. Biochim. Biophys. Acta, doi:10.1016/j.bbagen.2010.04.007.
Lee, H., Hoang, B., Fonge, H., Reilly, R.M., Allen, C., 2010. In vivo distribution of polymeric nanoparticles at the whole-body, tumor, and cellular levels. Pharm. Res. 27, 2343–2355.
Letchford, K., Burt, H., 2007. A review of the formation and classification of amphiphilic block copolymer nanoparticulate structures: micelles, nanospheres, nanocapsules and polymersomes. Eur. J. Pharm. Biopharm. 65, 259–269.
Letchford, K., Liggins, R., Burt, H., 2008. Solubilization of hydrophobic drugs by methoxy poly(ethylene glycol)-block-polycaprolactone diblock copolymer micelles: theoretical and experimental data and correlations. J. Pharm. Sci. 97, 1179–1190.
Leung, S.Y., Jackson, J., Miyake, H., Burt, H., Gleave, M.E., 2000. Polymeric micellar paclitaxel phosphorylates Bcl-2 and induces apoptotic regression of androgen-independent LNCaP prostate tumors. Prostate 44, 156–163.
Li, C., Wallace, S., 2008. Polymer-drug conjugates: recent development in clinical oncology. Adv. Drug Deliv. Rev. 60, 886–898.
Liggins, R.T., Hunter, W.L., Burt, H.M., 1997. Solid-state characterization of paclitaxel. J. Pharm. Sci. 86, 1458–1463.
Mugabe, C., Hadaschik, B.A., Kainthan, R.K., Brooks, D.E., So, A.I., Gleave, M.E., Burt, H.M., 2009. Paclitaxel incorporated in hydrophobically derivatized hyper-

branched polyglycerols for intravesical bladder cancer therapy. BJU Int. 103, 978–986.
Otova, B., Vaclavikova, R., Danielova, V., Holubova, J., Ehrlichova, M., Horsky, S., Soucek, P., Simek, P., Gut, I., 2006. Effects of paclitaxel, docetaxel and their combinations on subcutaneous lymphomas in inbred Sprague-Dawley/Cub rats. Eur. J. Pharm. Sci. 29, 442–450.
Pazdur, R., Kudelka, A.P., Kavanagh, J.J., Cohen, P.R., Raber, M.N., 1993. The taxoids: paclitaxel (Taxol) and docetaxel (Taxotere). Cancer Treat. Rev. 19, 351–386.
Qi, R., Gao, Y., Tang, Y., He, R.R., Liu, T.L., He, Y., Sun, S., Li, B.Y., Li, Y.B., Liu, G., 2009. PEG-conjugated PAMAM dendrimers mediate efficient intramuscular gene expression. AAPS J. 11, 395–405.
Ramaswamy, M., Zhang, X., Burt, H.M., Wasan, K.M., 1997. Human plasma distribution of free paclitaxel and paclitaxel associated with diblock copolymers. J. Pharm. Sci. 86, 460–464.
Rangel, C., Niell, H., Miller, A., Cox, C., 1994. Taxol and taxotere in bladder cancer: in vitro activity and urine stability. Cancer Chemother. Pharmacol. 33, 460–464.
Rosenberg, R., Devenney, W., Siegel, S., Dan, N., 2007. Anomalous release of hydrophilic drugs from poly(epsilon-caprolactone) matrices. Mol. Pharm. 4, 943–948.
Savic, R., Luo, L., Eisenberg, A., Maysinger, D., 2003. Micellar nanocontainers distribute to defined cytoplasmic organelles. Science 300, 615–618.
Sheikh, F.A., Barakat, N.A., Kanjwal, M.A., Aryal, S., Khil, M.S., Kim, H.Y., 2009. Novel self-assembled amphiphilic poly(epsilon-caprolactone)-grafted-poly(vinyl alcohol) nanoparticles: hydrophobic and hydrophilic drugs carrier nanoparticles. J. Mater. Sci. Mater. Med. 20, 821–831.
Singer, J.W., 2005. Paclitaxel poliglumex (XYOTAX, CT-2103): a macromolecular taxane. J. Control. Release 109, 120–126.
Sparreboom, A., Scripture, C.D., Trieu, V., Williams, P.J., De, T., Yang, A., Beals, B., Figg, W.D., Hawkins, M., Desai, N., 2005. Comparative preclinical and clinical pharmacokinetics of a cremophor-free, nanoparticle albumin-bound paclitaxel (ABI-007) and paclitaxel formulated in Cremophor (Taxol). Clin. Cancer Res. 11, 4136–4143.
Stiriba, S.E., Kautz, H., Frey, H., 2002. Hyperbranched molecular nanocapsules: comparison of the hyperbranched architecture with the perfect linear analogue. J. Am. Chem. Soc. 124, 9698–9699.
Straubinger, R.M., Balasubramanian, S.V., 2005. Preparation and characterization of taxane-containing liposomes. Methods Enzymol. 391, 97–117.
Stutz, H., 1995. The glass temperature of dendritic polymers. J. Polymer Sci. Part B: Polymer Phys. 33, 333–340.
Tanaka, M., Obata, T., Sasaki, T., 1996. Evaluation of antitumour effects of docetaxel (Taxotere) on human gastric cancers in vitro and in vivo. Eur. J. Cancer 32A, 226–230.
ten Tije, A.J., Verweij, J., Loos, W.J., Sparreboom, A., 2003. Pharmacological effects of formulation vehicles: implications for cancer chemotherapy. Clin. Pharmacokinet. 42, 665–685.
Tian, J., Stella, V.J., 2008a. Degradation of paclitaxel and related compounds in aqueous solutions I: epimerization. J. Pharm. Sci. 97, 1224–1235.
Tian, J., Stella, V.J., 2008b. Degradation of paclitaxel and related compounds in aqueous solutions II: Nonepimerization degradation under neutral to basic pH conditions. J. Pharm. Sci. 97, 3100–3108.
Tian, J., Stella, V.J., 2010. Degradation of paclitaxel and related compounds in aqueous solutions III: degradation under acidic pH conditions and overall kinetics. J. Pharm. Sci. 99, 1288–1298.
Turk, H., Shukla, A., Alves Rodrigues, P.C., Rehage, H., Haag, R., 2007. Water-soluble dendritic core-shell-type architectures based on polyglycerol for solubilization of hydrophobic drugs. Chemistry 13, 4187–4196.
Tziveleka, L.A., Kontoyianni, C., Sideratou, Z., Tsiourvas, D., Paleos, C.M., 2006. Novel functional hyperbranched polyether polyols as prospective drug delivery systems. Macromol. Biosci. 6, 161–169.
Verweij, J., Clavel, M., Chevalier, B., 1994. Paclitaxel (Taxol) and docetaxel (Taxotere): not simply two of a kind. Ann. Oncol. 5, 495–505.
Wilms, D., Stiriba, S.E., Frey, H., 2010. Hyperbranched polyglycerols: from the controlled synthesis of biocompatible polyether polyols to multipurpose applications. Acc. Chem. Res. 43, 129–141.
Zhang, L., Radovic-Moreno, A.F., Alexis, F., Gu, F.X., Basto, P.A., Bagalkot, V., Jon, S., Langer, R.S., Farokhzad, O.C., 2007. Co-delivery of hydrophobic and hydrophilic drugs from nanoparticle-aptamer bioconjugates. ChemMedChem 2, 1268–1271.
Zhang, X., Burt, H.M., Von Hoff, D., Dexter, D., Mangold, G., Degen, D., Oktaba, A.M., Hunter, W.L., 1997. An investigation of the antitumour activity and biodistribution of polymeric micellar paclitaxel. Cancer Chemother. Pharmacol. 40, 81–86.
Zhu, S., Hong, M., Tang, G., Qian, L., Lin, J., Jiang, Y., Pei, Y., 2010. Partly PEGylated polyamidoamine dendrimer for tumor-selective targeting of doxorubicin: the effects of PEGylation degree and drug conjugation style. Biomaterials 31, 1360–1371.
Zoli, W., Flamigni, A., Frassineti, G.L., Bajorko, P., De Paola, F., Milandri, C., Amadori, D., Gasperi-Campani, A., 1995. In vitro activity of taxol and taxotere in comparison with doxorubicin and cisplatin on primary cell cultures of human breast cancers. Breast Cancer Res. Treat. 34, 63–69.